

PACS: 13.75.Cs.; 14.20.Gk.; 13.30.Eg.

## Proposal for Studying $N^*$ Resonances with $\bar{p}p \rightarrow \bar{p}n\pi^+$ Reaction

Jia-Jun Wu,<sup>1,2</sup> Zhen Ouyang<sup>2,3</sup> and B. S. Zou<sup>1,2</sup>

<sup>1</sup> Institute of High Energy Physics, CAS, P.O.Box 918(4), Beijing 100049, China

<sup>2</sup> Theoretical Physics Center for Science Facilities, CAS, Beijing 100049, China

<sup>3</sup> Institute of Modern Physics, CAS, Lanzhou 730000, China

(Dated: September 8, 2009)

### Abstract

A theoretical study of the  $\bar{p}p \rightarrow \bar{p}n\pi^+$  reaction for antiproton beam energy from 1 to 4 GeV is made by including contributions from various known  $N^*$  and  $\Delta^*$  resonances. It is found that for the beam energy around 1.5 GeV, the contribution of the Roper resonance  $N_{(1440)}^*$  produced by the t-channel  $\sigma$  exchange dominates over all other contributions. Since such a reaction can be studied in the forthcoming  $\bar{P}$ ANDA experiment at the GSI Facility of Antiproton and Ion Research (FAIR), the reaction will be realistically the cleanest place for studying the properties of the Roper resonance and the best place for looking for other “missing”  $N^*$  resonances with large coupling to  $N\sigma$ .

## I. INTRODUCTION

The study of  $N^*$  resonances can provide us with critical insight into the nature of QCD in the confinement domain [1]. In the study of the  $N^*$  resonances, there are two long-standing central issues. First, many  $N^*$  states predicted by quark models have not been observed in experiments [2, 3, 4, 5], *i.e.*, so-called missing  $N^*$  problem. Second, the properties of the lowest well-established  $N^*$  resonances,  $N_{(1440)}^*$  and  $N_{(1535)}^*$ , are still not well determined experimentally [6] and not well understood theoretically [3].

As the lowest excited nucleon state, the Roper resonance  $N_{(1440)}^*$  was first deduced by  $\pi N$  phase shift analysis; its structure has been arousing people's interests intensely all the time; *i.e.*, it is lighter than the first odd-parity nucleon excitation, the  $N_{(1535)}^*$ , and has a significant branching ratio into two pions. Up to now, although the existence of the Roper resonance is well established (four-star ranking in the particle data book), its properties, such as mass, width, and decay branching ratios, still suffer large experiment uncertainties [6]. There are many models on this Roper resonance. In classical quark models, the Roper resonance has been associated with the first spin-parity  $J^P = 1/2^+$  radial excited state of the nucleon [5, 7, 8, 9]. In the bag [10] and Skyrme models [11], it was interpreted as surface oscillation, also called breathing mode. It has also been predicted as a monopole excitation of the nucleon with the gluonic excitation [12, 13, 14] or as dynamically generated from meson-nucleon interactions [15, 16]. But these predictions always reach either a larger value for its mass or a much smaller one for its width and also meet difficulties in explaining its electromagnetic coupling [17].

Up to now, our knowledge on  $N^*$  resonances has been mainly coming from  $\pi N$  and  $\gamma N$  experiments. Then those unobserved missing  $N^*$  resonances may be due to their weak couplings to  $\pi N$  and  $\gamma N$ . Even for the well-established Roper resonance, its properties can be extracted only by detailed partial-wave analysis. No corresponding peak has been observed from the  $\pi N$  invariant mass spectrum because of its nearby strong  $\Delta$  peak. A difficulty in extracting the  $N^*$  information from these experiments is the isospin decomposition of 1/2 and 3/2 [18]. Recently, the  $J/\psi \rightarrow \bar{N}N\pi$  and  $pp \rightarrow pn\pi^+$  reactions have been used to study  $N^*$  resonances with claimed observation of the Roper resonance peak [19, 20] due to their isospin filter effect [21, 22]. However, because of the presence of large interfering contributions from other resonances, there is still considerable model dependence in extracting its

properties. Moreover, the data [20] from  $pp \rightarrow pn\pi^+$  reaction are based on a preliminary analysis of the limited phase space, suffering a strong model dependence, and may have changed quite a bit in the course of the analysis, as suggested in a more recent paper by the same collaboration [23].

In this work, we propose to study the Roper and other  $N^*$  resonances with the  $\bar{p}p \rightarrow \bar{p}n\pi^+$  reaction, where thanks to the absence of the  $\Delta^{++}$  state, the contribution of the  $\Delta$  excitation is much smaller than that in the  $pp \rightarrow pn\pi^+$  reaction. It is found that for the beam energy around 1.5 GeV, the contribution of the Roper resonance  $N_{(1440)}^*$  produced by the t-channel  $\sigma$  exchange dominates over all other contributions because of its known large coupling to  $N\sigma$  [6, 24]. This will provide the cleanest place for studying the properties of the Roper resonance and the best place for looking for other missing  $N^*$  resonances with large coupling to  $N\sigma$ .

Such a reaction can be studied by the scheduled experiments on the Proton Antiproton Detector Array (PANDA) at the GSI Facility for Antiproton and Ion Research (FAIR) with the antiproton beam of kinetic energy ranging from 1 to 15 GeV [25]. The detector with an almost  $4\pi$  detection coverage for both charged particles and photons can detect  $\pi^+$  and  $\bar{p}$  in the final state. The neutron can be reconstructed from a missing mass spectrum against the  $\pi^+$  and  $\bar{p}$ . Hence we suggest the PANDA Collaboration pay good attention to the study of  $N^*$  resonances, considering its unique advantages found in this work.

In the next section, we present the formalism and ingredients for the calculation of the  $\bar{p}p \rightarrow \bar{p}n\pi^+$  reaction by including various intermediate  $N^*$  and  $\Delta^*$  resonances. Then in the Sec.III we give the numerical results of the calculation, compare this reaction to the  $pp \rightarrow pn\pi^+$  reaction, and discuss the results.

## II. FORMALISM AND INGREDIENTS

We study the  $\bar{p}p \rightarrow \bar{p}n\pi^+$  reaction within an effective Lagrangian approach. All the basic Feynman diagrams involved in our calculation for this reaction are depicted in Fig. 1. The formalism and ingredients are very similar to those used in the study of the  $pp \rightarrow pn\pi^+$  reaction [22], where only  $N_{(1440)}^*$ ,  $N_{(1520)}^*$ ,  $N_{(1680)}^*$  and  $\Delta_{(1232)}$  resonances are found to play significant roles for the beam energy around  $T_p = 1 \sim 3$  GeV. With the experience on the  $pp \rightarrow pn\pi^+$  reaction, we investigate here the contribution from these resonances to the

present  $\bar{p}p \rightarrow \bar{p}n\pi^+$  reaction for the beam energy  $T_{\bar{p}} = 1 \sim 4$  GeV.

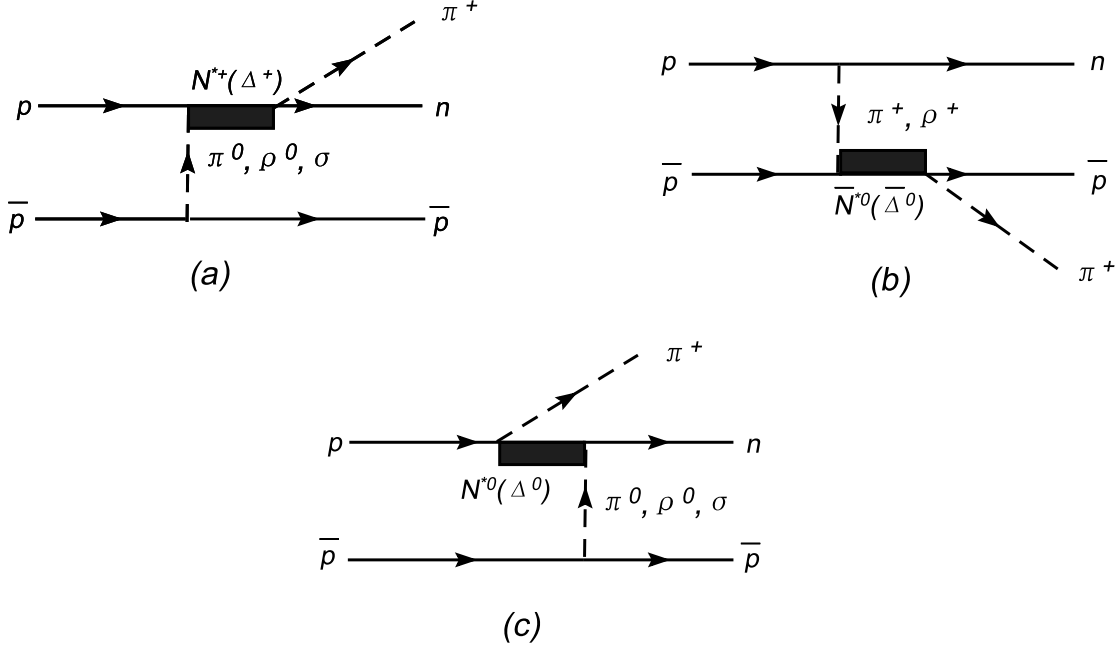


FIG. 1: Feynman diagrams of the  $\bar{p}p \rightarrow \bar{p}n\pi^+$  reaction.

First, we give the effective Lagrangian densities for describing the meson- $NN$  vertices:

$$\mathcal{L}_{\pi NN} = g_{\pi NN} \bar{u}_N \gamma_5 \vec{\tau} \cdot \vec{\psi}_\pi u_N + h.c., \quad (1)$$

$$\mathcal{L}_{\sigma NN} = g_{\sigma NN} \bar{u}_N \psi_\sigma u_N + h.c., \quad (2)$$

$$\mathcal{L}_{\rho NN} = g_{\rho NN} \bar{u}_N \left( \gamma_\mu + \frac{\kappa}{2m_N} \sigma_{\mu\nu} \partial^\nu \right) \vec{\tau} \cdot \vec{\psi}_\rho u_N + h.c. \quad (3)$$

Here  $\vec{\tau}$  is the usual isospin-1/2 Pauli matrix operator, and the coupling constants are all listed in Table I. At each vertex, we need a relevant off-shell form factor for the exchanged meson. In this paper, we use the same form factors as assumed in the previous literature [21, 22, 26, 27, 28, 29, 30]:

$$F_M^{NN}(k_M^2) = \left( \frac{\Lambda_M^2 - m_M^2}{\Lambda_M^2 - k_M^2} \right)^n. \quad (4)$$

Here  $M$  represents  $\pi$ ,  $\sigma$ , or  $\rho$  mesons. The  $\Lambda_M$  parameters as used in Refs.[21, 22] for the  $pp \rightarrow pn\pi^+$  reaction are also listed in Table I. Note that for  $NN$  elastic scattering, the square of the four-momentum vector  $k_M$  is equal to its corresponding three-momentum squared with a minus sign; hence, in some literature, such as in the Bonn model [30], an equivalent formula of the form factor with the three-momentum is used.

$M$	$n$	$g_{MNN}^2/4\pi$	$\Lambda_M(\text{GeV})$
$\pi$	1	14.4	1.3
$\sigma$	1	5.69	2.0
$\rho$	2	0.9 ( $\kappa = 6.1$ )	1.85

TABLE I: Coupling constants and cutoff parameters used for the meson- $NN$  vertices [21, 22].

Second, we consider the interaction vertices involving  $N^*$  and  $\Delta^*$  resonances. In Ref. [31], a Lorentz covariant orbital-spin scheme for  $N^*NM$  couplings is described in detail and can be easily extended to describe all the couplings appearing in the Feynman diagrams in Fig. 1. By using that scheme, the relevant important effective couplings [21, 22] are:

$$\mathcal{L}_{\pi N\Delta_{(1232)}} = g_{\pi N\Delta_{(1232)}} \bar{u}_N \partial^\mu \psi_\pi \tilde{\tau} u_{\Delta_{(1232)}\mu} + h.c., \quad (5)$$

$$\mathcal{L}_{\sigma NN^*_{(1440)}} = g_{\sigma NN^*_{(1440)}} \bar{u}_N \psi_\sigma u_{N^*_{(1440)}} + h.c., \quad (6)$$

$$\mathcal{L}_{\pi NN^*_{(1440)}} = g_{\pi NN^*_{(1440)}} \bar{u}_N \gamma_5 \gamma_\mu \vec{\tau} \cdot \partial^\mu \vec{\psi}_\pi u_{N^*_{(1440)}} + h.c., \quad (7)$$

$$\mathcal{L}_{\pi NN^*_{(1520)}} = g_{\pi NN^*_{(1520)}} \bar{u}_N \gamma_5 \gamma_\mu p_\pi^\mu p_\pi^\nu \vec{\tau} \cdot \vec{\psi}_\pi u_{N^*_{(1520)}\nu} + h.c., \quad (8)$$

$$\mathcal{L}_{\rho NN^*_{(1520)}} = g_{\rho NN^*_{(1520)}} \bar{u}_N \vec{\tau} \cdot \vec{\psi}_\rho u_{N^*_{(1520)}\mu} + h.c., \quad (9)$$

$$\mathcal{L}_{\pi NN^*_{(1680)}} = g_{\pi NN^*_{(1680)}} \bar{u}_N \gamma_5 \gamma_\mu p_\pi^\mu p_\pi^\nu p_\pi^\lambda \vec{\tau} \cdot \vec{\psi}_\pi u_{N^*_{(1680)}\nu\lambda} + h.c.. \quad (10)$$

Here  $\tilde{\tau}$  is the  $\frac{1}{2} \leftrightarrow \frac{3}{2}$  isospin transition operator. For the t-channel exchanged meson attached to every  $N^*$  and  $\Delta$  resonance, we also need the off-shell form factor:

$$F_M^{NR}(k_M^2) = \left( \frac{(\Lambda_M^R)^2 - m_M^2}{(\Lambda_M^R)^2 - k_M^2} \right)^n. \quad (11)$$

where  $R$  is  $N^*$  or  $\Delta$ . For the s-channel baryon resonances in Figs. 1(a) and 1(b) or u-channel baryon resonances in Fig. 1(c) we use the off-shell form factor [32, 33, 34]

$$F_R(q^2) = \frac{\Lambda^4}{\Lambda^4 + (q^2 - m_R^2)^2} \quad (12)$$

with  $\Lambda = 0.8\text{GeV}$ .

Although only the resonances and the meson exchanges listed in Table II are included in our present calculation, the results will not change much if all other  $N^*$  and  $\Delta^*$  resonances with spin-parity  $1/2^\pm$ ,  $3/2^\pm$  and  $5/2^\pm$  listed in the PDG [6] or other meson exchanges are also included, according to results from Ref. [22] for the  $pp \rightarrow pn\pi^+$  reaction.

The coupling constants of resonances can be obtained from their experimentally observed partial decay widths. For example, the  $g_{N^*_{(1440)}N\pi^0}$  can be obtained by the formula:

$$\Gamma_{N^*_{(1440)} \rightarrow N\pi} = \frac{g_{N^*_{(1440)}N\pi^0}^2 p_N^{c.m.}}{4\pi} \left[ \frac{m_\pi^2 (E_N - m_N)}{m_{N^*_{(1440)}}} + 2(p_N^{c.m.})^2 \right], \quad (13)$$

with

$$p_N^{c.m.} = \sqrt{\frac{(m_{N^*_{(1440)}}^2 - (m_N + m_\pi)^2)(m_{N^*_{(1440)}}^2 - (m_N - m_\pi)^2)}{4m_{N^*_{(1440)}}^2}}, \quad (14)$$

$$E_N = \sqrt{(p_N^{c.m.})^2 + m_N^2}. \quad (15)$$

In Table II, we list all the coupling constants and  $\Lambda_M^R$  parameters used in the calculation.

Third, we give the propagators of relevant particles. For the  $\pi$ ,  $\sigma$ , and  $\rho$  mesons, their propagators are simple:

$$G_{\pi(q)} = \frac{1}{q^2 - m_\pi^2}, \quad (16)$$

$$G_{\sigma(q)} = \frac{1}{q^2 - m_\sigma^2}, \quad (17)$$

$$G_{\rho(q)} = \frac{-\tilde{g}_{\mu\nu}}{q^2 - m_\rho^2}. \quad (18)$$

For the  $N^*$  and  $\Delta$  resonances, they are spin-1/2, spin-3/2, and spin-5/2 resonances. In addition, we must consider their antiparticles. The general formulas for the propagator of a half-integral spin particle is [35, 36]

$$G_{R(q)}^{n+\frac{1}{2}(\pm)} = \frac{P_{\mu_1\mu_2\dots\mu_n\nu_1\nu_2\dots\nu_n}^{n+\frac{1}{2}(\pm)}}{q^2 - m_R^2 + im_R\Gamma_R}, \quad (19)$$

$$P_{\mu_1\mu_2\dots\mu_n\nu_1\nu_2\dots\nu_n}^{n+\frac{1}{2}(\pm)} = \frac{n+1}{2n+3} (\not{p} \pm m) \gamma^\alpha \gamma^\beta P_{\alpha\mu_1\mu_2\dots\mu_n\beta\nu_1\nu_2\dots\nu_n}^{n+1}, \quad (20)$$

$$\begin{aligned} P_{\mu_1\mu_2\dots\mu_n\nu_1\nu_2\dots\nu_n}^n &= \left(\frac{1}{n!}\right)^2 \sum_{P(\mu)P(\nu)} \left[ \prod_{i=1}^n P_{\mu_i\nu_i} + a_1 P_{\mu_1\mu_2} P_{\nu_1\nu_2} \prod_{i=3}^n P_{\mu_i\nu_i} + \dots \right. \\ &\quad \left. + a_r P_{\mu_1\mu_2} P_{\nu_1\nu_2} P_{\mu_3\mu_4} P_{\nu_3\nu_4} \dots P_{\mu_{2r-1}\mu_{2r}} P_{\nu_{2r-1}\nu_{2r}} \prod_{i=2r+1}^n P_{\mu_i\nu_i} + \dots \right. \\ &\quad \left. + \begin{cases} a_{n/2} P_{\mu_1\mu_2} P_{\nu_1\nu_2} \dots P_{\mu_{n-1}\mu_n} P_{\nu_{n-1}\nu_n} & (\text{for even } n) \\ a_{(n-1)/2} P_{\mu_1\mu_2} P_{\nu_1\nu_2} \dots P_{\mu_{n-2}\mu_{n-1}} P_{\nu_{n-2}\nu_{n-1}} & (\text{for odd } n) \end{cases} \right], \quad (21) \end{aligned}$$

$$a_{r(n)} = \left(-\frac{1}{2}\right)^r \frac{n!}{r!(n-2r)!(2n-1)(2n-3)\dots(2n-2r+1)}. \quad (22)$$

From these formulas, the propagators of the relevant half-integral spin particles can be obtained explicitly as follows:

$$G_{R(q)}^{\frac{1}{2}(\pm)} = \frac{(\not{p} \pm m)}{q^2 - m_R^2 + im_R\Gamma_R}, \quad (23)$$

$$G_{R(q)}^{\frac{3}{2}(\pm)} = \frac{(\not{p} \pm m)}{q^2 - m_R^2 + im_R\Gamma_R} \left( -g_{\mu\nu} + \frac{1}{3}\gamma_\mu\gamma_\nu + \frac{2}{3}\frac{q_\mu q_\nu}{q^2} \pm \frac{1}{3m_R}(\gamma_\mu q_\nu - \gamma_\nu q_\mu) \right), \quad (24)$$

$$G_{R(q)}^{\frac{5}{2}(\pm)} = \frac{(\not{p} \pm m)}{q^2 - m_R^2 + im_R\Gamma_R} \left[ \frac{1}{2}(\tilde{g}_{\mu_1\nu_1}\tilde{g}_{\mu_2\nu_2} + \tilde{g}_{\mu_1\nu_2}\tilde{g}_{\mu_2\nu_1}) - \frac{1}{5}\tilde{g}_{\mu_1\nu_2}\tilde{g}_{\mu_1\nu_1} \right. \\ \left. - \frac{1}{10}(\tilde{\gamma}_{\mu_1}\tilde{\gamma}_{\nu_1}\tilde{g}_{\mu_2\nu_2} + \tilde{\gamma}_{\mu_1}\tilde{\gamma}_{\nu_2}\tilde{g}_{\mu_2\nu_1} + \tilde{\gamma}_{\mu_2}\tilde{\gamma}_{\nu_1}\tilde{g}_{\mu_1\nu_2} + \tilde{\gamma}_{\mu_2}\tilde{\gamma}_{\nu_2}\tilde{g}_{\mu_1\nu_1}) \right], \quad (25)$$

$$\tilde{\gamma}_\nu = \gamma_\nu - \frac{q_\nu \not{q}}{q^2}, \quad \tilde{g}_{\mu\nu} = g_{\mu\nu} - \frac{q_\mu q_\nu}{q^2}. \quad (26)$$

Here  $\pm$  means particle and antiparticle, respectively. We list the values for the widths ( $\Gamma_R$ ) and branching ratios of the included  $N^*$  and  $\Delta$  resonances in Table II.

$R$	$n$	$\Gamma_R(GeV)$	Decay mode	Branching ratios	$g^2/4\pi$	$\Lambda_M^R(GeV)$
$\Delta_{(1232)}$	2	0.118	$N\pi$	1.0	19.54	0.6
$N_{(1440)}^*$	1	0.3	$N\pi$	0.65	1.53	1.3
			$N\sigma$	0.075	3.20	1.1
$N_{(1520)}^*$	1	0.115	$N\pi$	0.6	5.19	0.8
			$N\rho$	0.09	3.96	0.8
$N_{(1680)}^*$	1	0.13	$N\pi$	0.675	16.59	0.8

TABLE II: Resonances and parameters used in the calculation. Widths and branching ratios are from PDG [6]; cutoff parameters are from Refs. [21, 22, 26, 27].

With all relevant effective Lagrangians, coupling constants, and propagators fixed, the amplitudes for various diagrams can be written straightforwardly by following the Feynman rules. And the total amplitude is just their simple sum. Here we give explicitly the individual amplitudes corresponding to  $N_{(1440)}^{*+}\pi^0$ ,  $N_{(1440)}^{*0}\pi^0$  and  $\bar{N}_{(1440)}^{*0}\pi^+$  for the Feynman diagrams

(a), (c), and (b) in Fig.1, as an example,

$$\begin{aligned}
\mathcal{M}_{N_{(1440)}^* \pi^0} &= \mathcal{M}_{N_{(1440)}^{*+} \pi^0} + \mathcal{M}_{N_{(1440)}^{*0} \pi^0} \\
&= \frac{\sqrt{2}}{3} \left( \bar{u}_{p_n s_n} \gamma_5 \not{p}_{\pi^+} G_{N_{(1440)}^*}^{(\frac{1}{2})^+} F_{N_{(1440)}^*}(q^2) \not{k}_{\pi^0} u_{p_p s_p} + \bar{u}_{p_n s_n} \not{k}_{\pi^0} G_{N_{(1440)}^*}^{(\frac{1}{2})^+} F_{N_{(1440)}^*}(q^2) \not{p}_{\pi^+} u_{p_p s_p} \right) \\
&\quad \times g_{\pi NN}^2 \frac{1}{k_{\pi^0}^2 - m_{\pi^0}^2} F_{\pi}^{NN^*}(k_{\pi^0}^2) F_{\pi}^{NN}(k_{\pi^0}^2) g_{NN\pi} \bar{v}_{p_{\bar{p}_1} s_{\bar{p}_1}} \gamma_5 v_{p_{\bar{p}_2} s_{\bar{p}_2}}, \tag{27}
\end{aligned}$$

$$\begin{aligned}
\mathcal{M}_{\bar{N}_{(1440)}^* \pi^+} &= \frac{2\sqrt{2}}{3} g_{\pi NN}^2 \bar{v}_{p_{\bar{p}_1} s_{\bar{p}_1}} \gamma_5 \not{p}_{\pi^+} G_{\bar{N}_{(1440)}^*}^{(\frac{1}{2})^-} F_{N_{(1440)}^*}(q^2) \not{k}_{\pi^+} v_{p_{\bar{p}_2} s_{\bar{p}_2}} \frac{1}{k_{\pi^+}^2 - m_{\pi^+}^2} \\
&\quad \times F_{\pi}^{NN^*}(k_{\pi^+}^2) F_{\pi}^{NN}(k_{\pi^+}^2) g_{NN\pi} \bar{u}_{p_n s_n} \gamma_5 u_{p_p s_p}, \tag{28}
\end{aligned}$$

where  $u_{p_n s_n}$ ,  $v_{p_{\bar{p}_2} s_{\bar{p}_2}}$ ,  $u_{p_p s_p}$ , and  $v_{p_{\bar{p}_1} s_{\bar{p}_1}}$  denote the spin wave functions of the outgoing neutron, antiproton in the final state and initial proton and antiproton, respectively.  $p_{\pi^+}$ ,  $k_{\pi^+}$ , and  $k_{\pi^0}$  are the four-momenta of the outgoing and the exchanged pion mesons.  $q$  is the four-momenta of the  $N^*$ .  $p_p$  and  $p_{\bar{p}_1}$  represent the four-momenta of the initial proton and antiproton.  $p_n$  and  $p_{\bar{p}_2}$  represent the four-momenta of the final neutron and antiproton. And factor  $\sqrt{2}/3$  and  $2\sqrt{2}/3$  are from isospin  $C - G$  coefficients.

So the total amplitude of the  $\bar{p}p \rightarrow \bar{p}n\pi^+$  reaction can be obtained as

$$\begin{aligned}
\mathcal{M}_{\bar{p}p \rightarrow \bar{p}n\pi^+} &= \mathcal{M}_{p\pi^0} + \mathcal{M}_{\bar{n}\pi^+} + \mathcal{M}_{N_{(1440)}^* \pi^0} + \mathcal{M}_{\bar{N}_{(1440)}^* \pi^+} + \mathcal{M}_{N_{(1440)}^* \sigma} \\
&\quad + \mathcal{M}_{N_{(1520)}^* \pi^0} + \mathcal{M}_{\bar{N}_{(1520)}^* \pi^+} + \mathcal{M}_{N_{(1520)}^* \rho^0} + \mathcal{M}_{\bar{N}_{(1520)}^* \rho^+} \\
&\quad + \mathcal{M}_{N_{(1680)}^* \pi^0} + \mathcal{M}_{\bar{N}_{(1680)}^* \pi^+} + \mathcal{M}_{\Delta_{(1232)} \pi^0} + \mathcal{M}_{\bar{\Delta}_{(1232)}^0 \pi^+}. \tag{29}
\end{aligned}$$

Then the calculation of the cross section  $\sigma_{\bar{p}p \rightarrow \bar{p}n\pi^+}$  is straightforward:

$$\sigma_{\bar{p}p \rightarrow \bar{p}n\pi^+} = \frac{1}{4} \frac{m_p^2}{(2\pi)^5 \sqrt{(p_p \cdot p_{\bar{p}_1})^2 - m_p^2}} \sum_{s_i} \sum_{s_f} |\mathcal{M}_{\bar{p}p \rightarrow \bar{p}n\pi^+}|^2 d\phi, \tag{30}$$

$$d\phi = \frac{m_p d^3 p_{\bar{p}_2}}{E_{\bar{p}_2}} \frac{d^3 p_{\pi}}{2E_{\pi}} \frac{m_n d^3 p_n}{E_n} \delta^4(p_p + p_{\bar{p}_1} - p_n - p_{\pi} - p_{\bar{p}_2}). \tag{31}$$

### III. NUMERICAL RESULTS AND DISCUSSION

With the formalism and ingredients given in the former section, we compute the total cross section versus the kinetic energy of the antiproton beam  $T_{\bar{p}}$  for the  $\bar{p}p \rightarrow \bar{p}n\pi^+$  reaction for  $T_{\bar{p}} = 1 \sim 4$  GeV by using the code FOWL from the CERN program library, which is a program for Monte Carlo multiparticle phase-space integration weighted by the amplitude squared. The results are shown in Fig.2. The total cross section for the  $\bar{p}p \rightarrow \bar{p}n\pi^+$  reaction



reaches a maximum of about 10 mb at  $T_{\bar{p}}$  around 2.2 GeV. Compared with the  $\bar{p}p$  total cross section of about 90 mb and  $\bar{p}p$  elastic scattering cross section of about 30 mb around such energy [6], this is a rather large share of the  $\bar{p}p$  total cross section.

For the energies from 1 to 2.8 GeV, the largest contribution comes from the Roper  $N_{(1440)}^*$  excitation. It reaches maximum around 1.55 GeV, where it dominates over all other contributions. It is mainly produced by the t-channel  $\sigma$  exchange as shown in Fig. 2(d). This will provide a very clean place for studying properties of the Roper resonance, such as its mass, width, and coupling to  $N\sigma$ . The t-channel  $\sigma$  exchange is not only important for  $N_{(1440)}^*$  production, but also for the nucleon pole contribution, as shown in Fig.2(b). This suggests that the  $\bar{p}p$  reactions may provide a good place for looking for those missing  $N^*$  resonances with large coupling to  $N\sigma$ .

For the energy above 2.8 GeV, the contribution from  $N_{(1680)}^*$  takes over to be the largest one, produced mainly by t-channel pion exchange. For each  $N^*$  production with t-channel pion exchange, the contribution from  $\bar{N}^*$  is almost four times that from  $N^*$  because of the relevant  $C - G$  coefficients for Feynman diagrams in Figs. 1(a) and 1(b) except for  $N_{(938)}$  where the contribution of the Feynman diagram in Fig. 1(c) is comparable to those from Figs. 1(a) and 1(b). On the other hand, the t-channel  $\sigma$  exchange cannot produce  $\bar{N}^*$  to reach the  $\bar{p}n\pi^+$  final state. Therefore, the  $N^*$  mainly produced by t-channel pion exchange will show up most clearly in the  $\bar{p}\pi^+$  invariant mass spectrum, while those  $N^*$  mainly produced by t-channel  $\sigma$  exchange will show up clearly only in the  $n\pi^+$  invariant mass spectrum.

Here the contribution from  $\Delta$  excitation is small in contrast to the case of the  $pp \rightarrow pn\pi^+$  reaction, where the  $\Delta$  excitation gives the largest contribution [21, 22]. This is because the  $\Delta^{++}$  excitation in the  $pp \rightarrow pn\pi^+$  reaction is much more favored by the isospin  $CG$  coefficients than the  $\Delta^+$  and  $\bar{\Delta}^0$  excitations in the  $\bar{p}p \rightarrow \bar{p}n\pi^+$  reaction.

In Figs.3 and 4, we show the prediction of Dalitz plots and invariant mass spectra of  $\bar{p}\pi^+$  and  $n\pi^+$  for the  $\bar{p}p \rightarrow \bar{p}n\pi^+$  reaction compared with the corresponding ones for the  $pp \rightarrow pn\pi^+$  reaction [22] at  $T_{\bar{p}} = 1.55$  GeV (Fig.3) and 2.88 GeV (Fig.4).

At  $T_{\bar{p}} = 1.55$  GeV, for the  $\bar{p}p \rightarrow \bar{p}n\pi^+$  reaction, both the Dalitz plot and  $n\pi^+$  invariant mass spectrum show clear dominance of the  $N_{(1440)}^*$  resonance over other contributions. So this provides us with an excellent place to study the properties of the Roper resonance. In the  $\bar{p}\pi^+$  invariant mass spectrum, three peaks correspond to the  $\bar{\Delta}^0$ ,  $\bar{N}_{(1440)}^{*0}$ , and  $\bar{N}_{(1520)}^{*0}$ ,

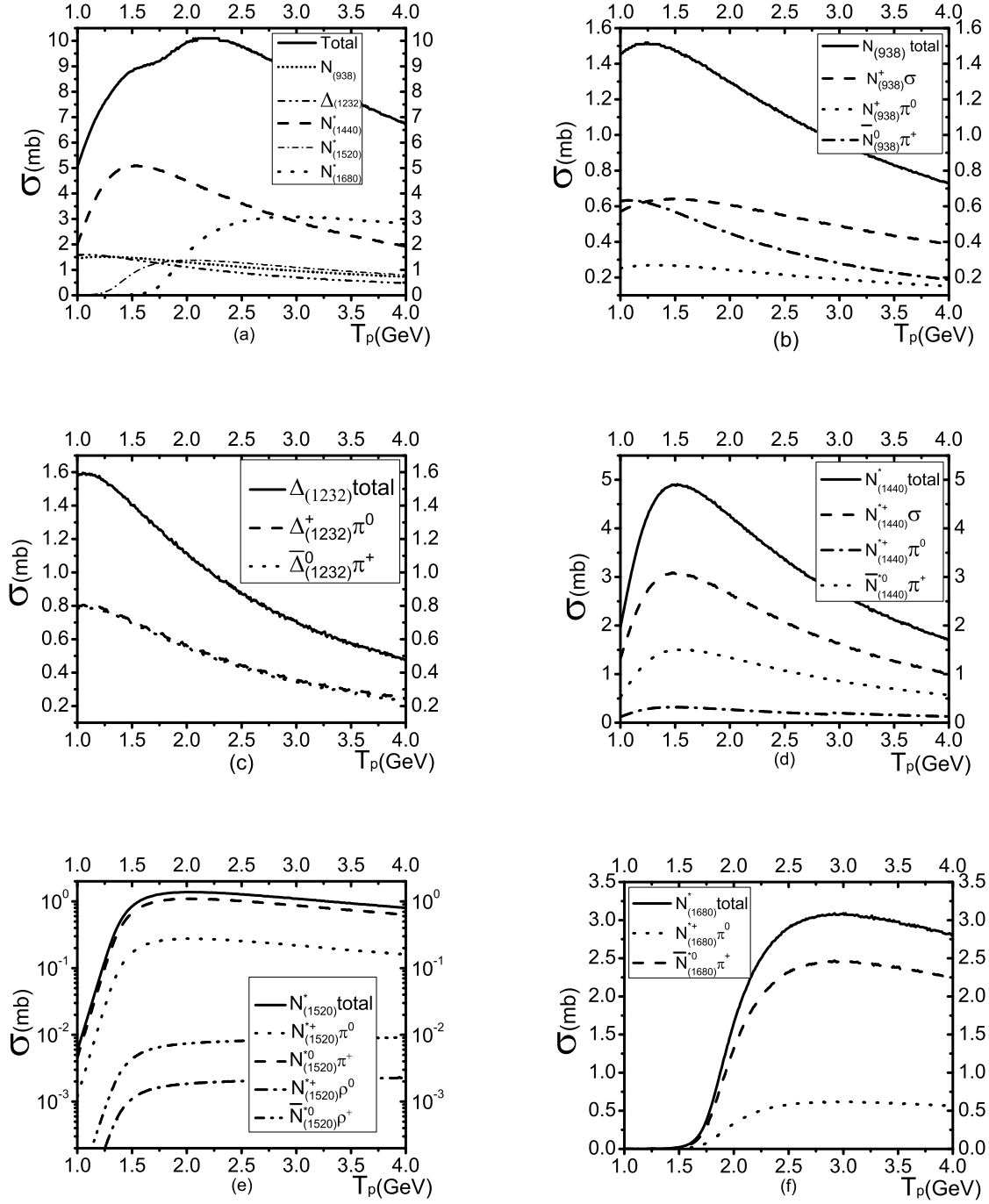


FIG. 2: Prediction of the cross section vs beam energy  $T_{\bar{p}}$  for the  $\bar{p}p \rightarrow \bar{p}n\pi^+$  reaction. (a) Total cross section and contributions from each resonance included. (b)-(f)  $N_{(938)}$ ,  $\Delta_{(1232)}$ ,  $N^*_{(1440)}$ ,  $N^*_{(1520)}$ , and  $N^*_{(1680)}$ , respectively, showing contributions from various Feynman diagrams for each resonance and their subtotal cross section.

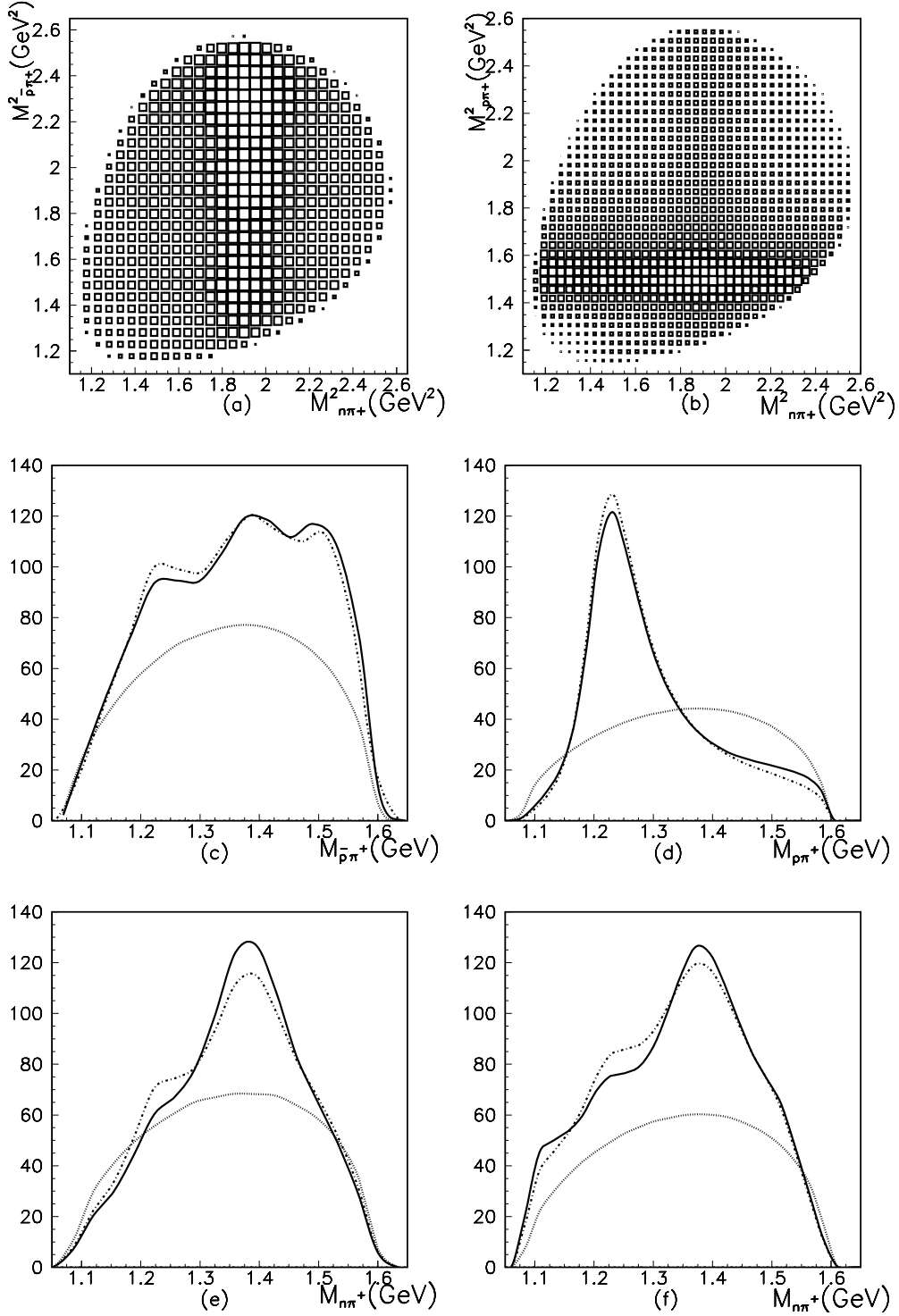


FIG. 3: Prediction of Dalitz plots and invariant mass spectra (solid curves) of  $\bar{p}\pi^+$  and  $n\pi^+$  for the  $\bar{p}p \rightarrow \bar{p}n\pi^+$  reaction (left column) compared with the corresponding ones for the  $pp \rightarrow pn\pi^+$  reaction (right column) [22] at  $T_{\bar{p}} = 1.55$  GeV. The dotted lines are results with some parameters replaced by those in Table.III. The dashed curves are phase-space distributions.

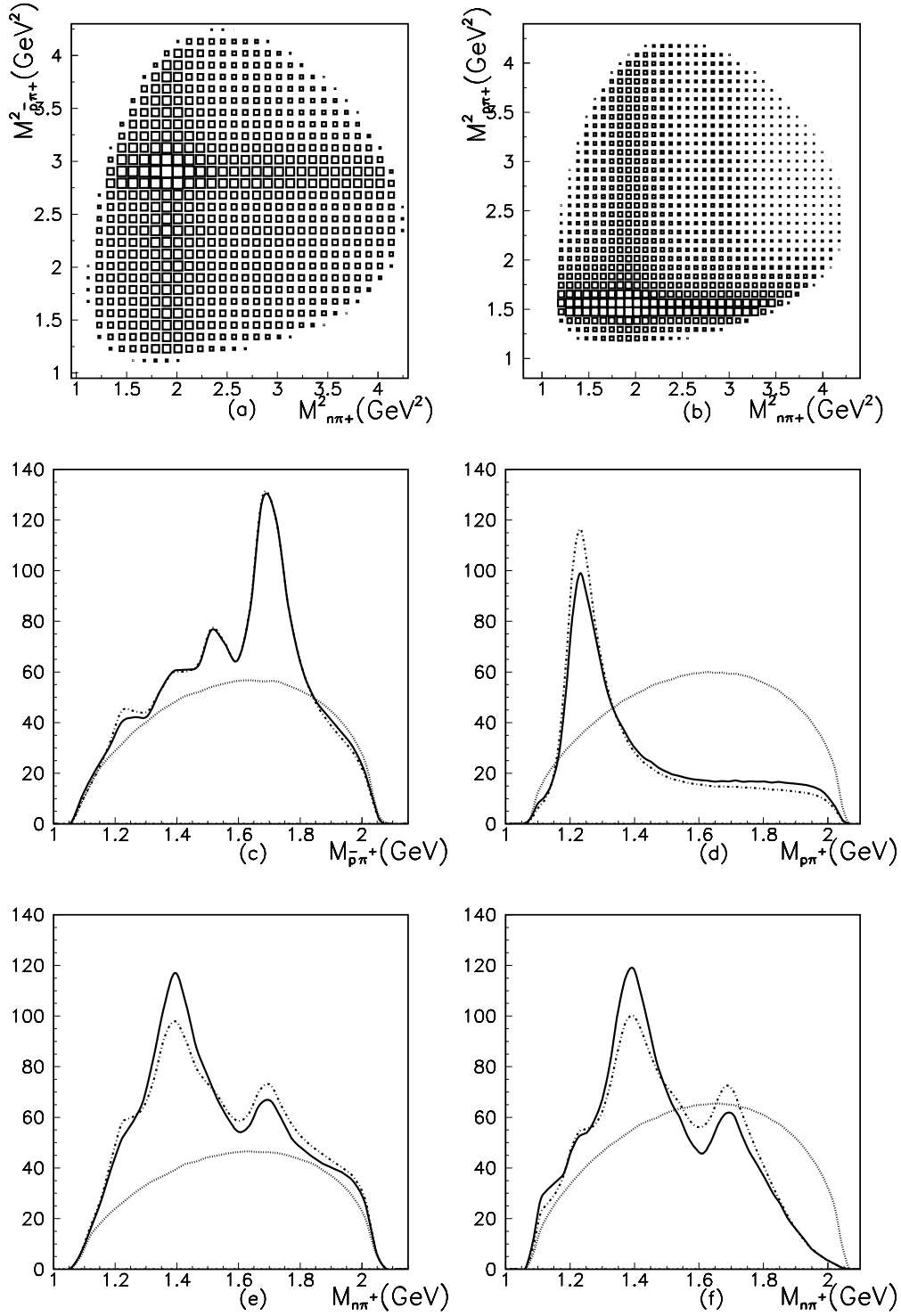


FIG. 4: Same as Fig. 3, but at  $T_{\bar{p}} = 2.88$  GeV.

respectively. In comparison, in the corresponding  $p\pi^+$  invariant mass spectrum for the  $pp \rightarrow pn\pi^+$  reaction, as shown in Fig.3(d), one can only see the clearly dominating  $\Delta^{++}$  peak, which shadows all other resonances. So the  $\bar{p}p \rightarrow \bar{p}n\pi^+$  reaction here provides also a chance to study some properties of  $N^*(1520)$ .

At  $T_{\bar{p}} = 2.88$  GeV, in the  $\bar{p}\pi^+$  invariant mass spectrum, a clear  $\bar{N}_{(1680)}^{*0}$  peak and small  $\bar{N}_{(1520)}^{*0}$ ,  $\bar{N}_{(1440)}^{*0}$ , and  $\bar{\Delta}^0$  peaks are visible. They are produced by the t-channel pion exchange and should have their  $N^{*+}$  partners making corresponding contributions to the  $n\pi^+$  invariant mass spectrum with a reduction factor of 4. However, because of the large  $N_{(1440)}^*$  production from the t-channel  $\sigma$  exchange, the  $N_{(1440)}^*$  peak dominates the  $n\pi^+$  invariant mass spectrum with a small  $N_{(1680)}^*$  peak in addition. Compared with the  $pp \rightarrow pn\pi^+$  reaction at the same energy, the  $n\pi^+$  invariant mass spectra are similar, whereas the  $\bar{p}\pi^+$  spectrum is very different from the  $p\pi^+$  spectrum where the  $\Delta^{++}$  peak overwhelmingly dominates because of its much more favorable isospin factor. For the  $\bar{p}p \rightarrow \bar{p}n\pi^+$  reaction, the  $\bar{N}^*$  peaks in the  $\bar{p}\pi^+$  spectrum put an additional constraint on  $N^*$  production from the t-channel pion exchange. This is an advantage for extracting  $N\sigma$  coupling of  $N^*$  produced in this reaction.

In our calculation, we have not included the  $\bar{p}p$  initial state interaction (ISI) and  $\bar{p}n$  final state interaction (FSI) factors. For the energies considered here,  $T_{\bar{p}} > 1$  GeV, which is well above the  $\bar{p}p$  threshold, the role of ISI is basically to reduce the cross section by an overall factor with little energy dependence [37, 38], and ISI can be equivalently absorbed into the adjustment of form factor parameters. This is why the  $\Delta N\pi$  form factor that we used is rather softer than those that include explicitly an additional ISI reduction factor. Note that the  $\bar{p}p$  elastic scattering cross sections for the beam energy  $T_{\bar{p}}$  in the range of  $1 \sim 4$  GeV are larger than the corresponding  $pp$  elastic scattering cross sections [6]. Then the ISI for  $\bar{p}p$  reaction seems not to give a stronger reduction than the corresponding  $pp$  reaction in this energy range. Assuming the same parameters as for the  $pp$  reaction should have given a reasonable estimation of cross sections for the corresponding  $\bar{p}p$  reaction. For such energies, only a small portion of  $\bar{p}n$  in the final state will be in the relative S wave and their FSI should not play a very important role. Usually, the FSI plays significant role only for near-threshold meson production.

All the above results are based on the parameters in the Table I and II taken from Refs. [21, 22], which reproduce well the data of the  $pp \rightarrow pn\pi^+$  reaction [20]. For the  $pp \rightarrow pn\pi^+$  reaction with beam energies in the range of  $1 \sim 4$  GeV, the two largest contributions

are found to be from the  $\Delta$  excitation with the t-channel  $\pi$  exchange and the  $N^*(1440)$  excitation from the t-channel  $\sigma$  exchange [21, 22]. The parameters for these two biggest contributions were adjusted to reproduce the data of Ref.[20], which demand significant production of the  $N^*(1440)$ . But since the data of Ref.[20] are preliminary and may not be very reliable [23], the constraint from the data on the parameters may also be unreliable. To provide an assessment of the uncertainties involved and their implications, we should check the results with parameters without constraint from the data of Ref.[20]. Some typical values for these parameters are listed in Table III. For the  $\Delta N\pi$  vertex form factor, the cutoff parameter 1.2 GeV with  $n = 1$  as in the Bonn model is a commonly used value [29, 30, 39]. However, with such a hard  $\Delta N\pi$  form factor, an ISI reduction factor about 0.19 is needed to reproduce the  $pp \rightarrow pn\pi^+$  total cross section. Without such an ISI factor, then a much softer  $\Delta N\pi$  form factor with cutoff parameter of about 0.65 GeV is needed to reproduce the data [40]. According to Ref.[40] any attempt to include the  $\rho$ -meson exchange worsens the agreement with experiments of  $pp \rightarrow n\Delta^{++}$ . Hence for the  $\Delta$  production, the  $\rho$ -meson exchange has been ignored in Refs.[21, 22] and here. Assuming the same parameters of the Bonn model with the ISI reduction factor of 0.19 for the  $\bar{p}p \rightarrow \bar{p}n\pi^+$  reaction, then the calculated contribution of  $\Delta$  production to the total cross section is shown by the dashed curve in Fig.5(a) and is about 50% larger than the result using the parameters of Ref.[22]. For the  $N_{(1440)}^* N\sigma$  coupling, the parameters in Table III are from Refs.[24, 41] which reproduced well the data on  $p\alpha \rightarrow p\alpha\pi\pi$  and  $pp \rightarrow NN\pi\pi$  reactions without including the ISI reduction factor. Assuming these parameters for the  $\bar{p}p \rightarrow \bar{p}n\pi^+$  reaction, then the calculated contribution of  $N_{(1440)}^*$  production to the total cross section is shown by the dashed curve in Fig.5(b) and is about 30% smaller than the result using the parameters of Ref.[22]. Note that the  $N_{(1440)}^* N\sigma$  coupling in Table III is much smaller than the value in Table II, which is determined from the PDG value for the  $N_{(1440)}^* \rightarrow N\sigma$  decay width. So one regards the  $N_{(1440)}^* N\sigma$  coupling in Table III as effectively including some ISI reduction factor.

Results with these parameters without adjustment to fit data from Ref.[20] are plotted for various mass spectra of the  $\bar{p}p \rightarrow \bar{p}n\pi^+$  reaction at  $T_{\bar{p}} = 1.55$  and 2.88 GeV, as shown by the dashed curves in Figs.3 and 4 as a comparison to those results (solid curves) with the parameters of Ref.[22]. Although quantitatively there are about 30%~50% uncertainty about the relative production rates of  $\Delta$  and  $N_{(1440)}^*$  resonances, qualitatively the main

$R$	$n$	$g^2/4\pi$	$\Lambda_M^R(\text{GeV})$	Source
$\Delta_{(1232)}N\pi$	1	19.54	1.2	[29, 30]
$N_{(1440)}^*N\sigma$	1	1.33	1.7	[24, 41]
$NN\sigma$	1	5.69	1.7	[29, 30, 41]

TABLE III: Parameters without adjustment to fit data from Ref.[20].

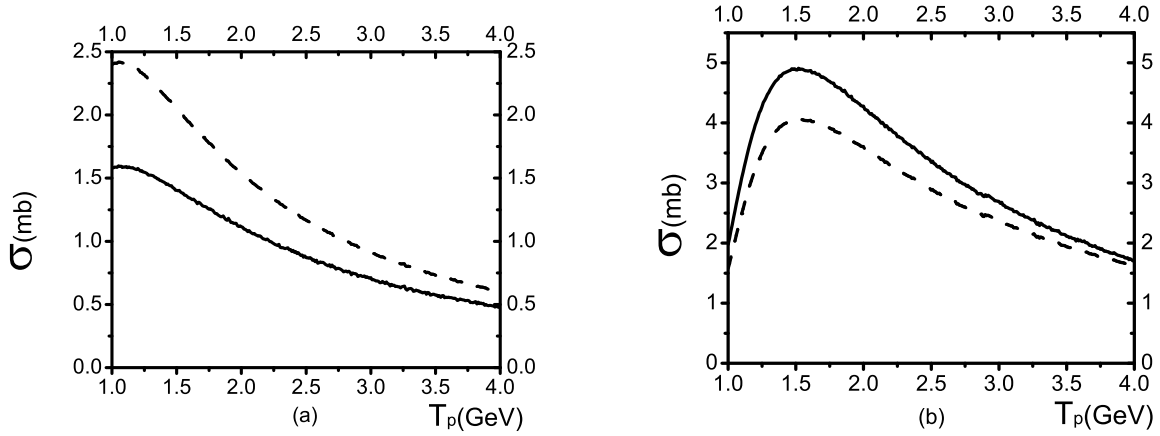


FIG. 5: Contribution of (a)  $\Delta$  and (b)  $N^*(1440)$  to the  $\bar{p}p \rightarrow \bar{p}n\pi^+$  total cross sections with two sets of parameters: the same parameters as in Ref.[22](solid curves) and some parameters replaced by those in Table.III(dashed curves).

conclusion of the study is rather firm, *i.e.*, the  $N^*(1440)$  should be clearly seen in the  $\bar{p}p \rightarrow \bar{p}n\pi^+$  reaction and dominates the reaction at  $T_{\bar{p}} = 1.55$  GeV.

With a clear advantage for studying  $N^*$  of the large  $N\sigma$  coupling by the  $\bar{p}p \rightarrow \bar{p}n\pi^+$  reaction, finally let us discuss the experimental accessibility of this reaction. We know that the  $\bar{p}p$  reaction will be studied by the PANDA (anti-Proton ANnihilation at DArmstadt) Collaboration at FAIR with the  $\bar{p}$  beam energy in the range of 1.5 to 15 GeV and luminosity of about  $10^{31} \text{cm}^{-2}\text{s}^{-1}$  [25]. For our proposed  $N^*$  study with the  $\bar{p}p \rightarrow \bar{p}n\pi^+$  reaction, the best beam energy range is 1.5-4 GeV, with a cross section around 8 mb, which corresponds to an event production rate of  $8 \times 10^5$  per second at PANDA/FAIR. The PANDA is supposed to be a  $4\pi$  solid angle detector with good particle identification for charged particles and photons. For the  $\bar{p}p \rightarrow \bar{p}n\pi^+$  reaction, if  $\pi^+$  and  $\bar{p}$  are identified, then the neutron can be

easily reconstructed from the missing mass spectrum against  $\pi^+$  and  $\bar{p}$ . So this reaction should be easy accessible at PANDA/FAIR.

In summary, we find that the  $\bar{p}p \rightarrow \bar{p}n\pi^+$  reaction provides an excellent place for studying properties of the Roper  $N^*(1440)$  resonance and any other  $N^*$  resonances (including some missing ones) with large couplings to  $N\sigma$ ; and the reaction is easily accessible by the forthcoming experiments at the PANDA/FAIR. With a large amount of data on the final states including baryon and antibaryon, the PANDA/FAIR could play an important role in the study of  $N^*$  and hyperon excited states.

**Acknowledgements** We thank Ju-Jun Xie for useful discussions. This work is partly supported by the National Natural Science Foundation of China (NSFC) under Grant Nos. 10875133, 10821063, 10635080, the Chinese Academy of Sciences (KJCX3-SYW-N2), and the Ministry of Science and Technology of China (2009CB825200).

- 
- [1] N. Isgur, arXiv:nucl-th/0007008.
  - [2] B. C. Liu and B. S. Zou, Commun. Theor. Phys. **46** (2006) 501.
  - [3] S. Capstick and W. Roberts, Prog. Part. Nucl. Phys. **45**, S241 (2000).
  - [4] S. Capstick and W. Roberts, Phys. Rev. D **47** (1993) 1994.
  - [5] N. Isgur and G. Karl, Phys. Rev. D **18** (1978) 4187; Phys. Rev. D **19** (1979) 2653 [Erratum-ibid. D **23** (1981) 817].
  - [6] C. Amsler *et al.* [Particle Data Group], Phys. Lett. B **667** (2008) 1.
  - [7] S. Capstick and N. Isgur, Phys. Rev. D **34** (1986) 2809.
  - [8] L. Y. Glozman, W. Plessas, K. Varga and R. F. Wagenbrunn, Phys. Rev. D **58** (1998) 094030.
  - [9] K. F. Liu and C. W. Wong, Phys. Rev. D **28** (1983) 170.
  - [10] U. G. Meissner and J. W. Durso, Nucl. Phys. A **430** (1984) 670.
  - [11] C. Hajduk and B. Schwesinger, Phys. Lett. B **140** (1984) 172.
  - [12] T. Barnes and F. E. Close, Phys. Lett. B **123** (1983) 89.
  - [13] E. Golowich, E. Haqq and G. Karl, Phys. Rev. D **28** (1983) 160; [**33** (1986) 859(E)].
  - [14] L. S. Kisslinger and Z. P. Li, Phys. Rev. D **51** (1995) R5986.
  - [15] O. Krehl, C. Hanhart, C. Krewald and J. Speth, Phys. Rev. C **62** (2000) 025207.
  - [16] C. Schutz, J. Haidenbauer, J. Speth and J. W. Durso, Phys. Rev. C **57** (1998) 1464.



- [17] A. V. Sarantsev *et al.*, Phys. Lett. B **659** (2008) 94.
- [18] R. Workman, Few Body Syst. Suppl. **11** (1999) 94.
- [19] M. Ablikim *et al.* [BES Collaboration], Phys. Rev. Lett. **97** (2006) 062001.
- [20] H. Clement *et al.*, arXiv:nucl-ex/0612015.
- [21] Z. Ouyang, J. J. Xie, B. S. Zou and H. S. Xu, Nucl. Phys. A **821**, 220 (2009)
- [22] Z. Ouyang, J. J. Xie, B. S. Zou and H. S. Xu, Int. J. Mod. Phys. E **18**, 281 (2009)
- [23] T. Skorodko *et al.*, Eur. Phys. J. A **35**, 317 (2008).
- [24] S. Hirenzaki, P. Fernandez de Cordoba and E. Oset, Phys. Rev. C **53** (1996) 277.
- [25] J. G. Messchendorp [PANDA Collaboration], *In Proceedings of the 11th International Conference on Meson-Nucleon Physics and the Structure of the Nucleon (MENU2007), Julich, Germany, 10-14 Sept. 2007, p. 123(unpublished)* [arXiv:0711.1598 [nucl-ex]]; K. T. Brinkmann, Nucl. Instrum. Meth. A **549**, 146 (2005).
- [26] J. J. Xie and B. S. Zou, Phys. Lett. B **649** (2007) 405; J. J. Xie, B. S. Zou and H. C. Chiang, Phys. Rev. C **77** (2008) 015206.
- [27] K. Tsushima, S. W. Huang and A. Faessler, Phys. Lett. B **337** (1994) 245; J. Phys. G **21** (1995) 33; K. Tsushima, A. Sibirtsev and A. W. Thomas, Phys. Lett. B **390** (1997) 29; K. Tsushima, A. Sibirtsev, A. W. Thomas, and G. Q. Li Phys. Rev. C **59** (1999) 369 [**61** (2000) 029903(E)].
- [28] A. Sibirtsev and W. Cassing, arXiv:nucl-th/9802019; A. Sibirtsev, K. Tsushima, W. Cassing and A. W. Thomas, Nucl. Phys. A **646** (1999) 427.
- [29] J. Haidenbauer, K. Holinde and A. W. Thomas, Phys. Rev. C **49**, 2331 (1994).
- [30] R. Machleidt, K. Holinde and C. Elster, Phys. Rept. **149** (1987) 1; R. Machleidt, Adv. Nucl. Phys. **19** (1989) 189.
- [31] B. S. Zou and F. Hussain, Phys. Rev. C **67** (2003) 015204.
- [32] G. Penner and U. Mosel, Phys. Rev. C **66** (2002) 055212; **66** (2002) 055211.
- [33] V. Shklyar, H. Lenske and U. Mosel, Phys. Rev. C **72** (2005) 015210.
- [34] T. Feuster and U. Mosel, Phys. Rev. C **58** (1998) 457; **59** (1999) 460.
- [35] R. E. Behrends and C. Fronsdal, Phys. Rev. **106** (1957) 345 .
- [36] S. Z. Huang, P. F. Zhang, T. N. Ruan, Y. C. Zhu and Z. P. Zheng, Eur. Phys. J. C **42** (2005) 375.
- [37] C. Hanhart, Phys. Rept. **397** (2004) 155.
- [38] V. Baru, A. M. Gasparyan, J. Haidenbauer, C. Hanhart, A. E. Kudryavtsev and J. Speth,

Phys. Rev. C **67** (2003) 024002

[39] B. K. Jain and A. B. Santra, Phys. Rev. C **46**, 1183 (1992); B. K. Jain and B. Kundu, *ibid.* **53**, 1917 (1996).

[40] B. Kundu, B. K. Jain and A. B. Santra, Phys. Rev. C **58**, 1614 (1998) [ C **61**, 049902(E) (2000)].

[41] E. Hernandez and E. Oset, Phys. Rev. C **60**, 025204 (1999).